*Inorg. Chem.* **2008**, *47*, 6220−6226


# Valence Electronic Structure of Benzo-2,1,3-chalcogenadiazoles Studied by Photoelectron Spectroscopy and Density Functional Theory

**Anthony F. Cozzolino,[†] Nadine E. Gruhn,[‡] Dennis L. Lichtenberger,[‡] and Ignacio Vargas-Baca*[,†]**

*McMaster University, 1280 Main Street West, Hamilton, ON L8S 4M1, Canada, and The University of Arizona, Tucson, Arizona 85721, USA*

Received January 11, 2008

The He I photoelectron spectra of benzo-2,1,3-thia-, selena-, and telluradiazole were measured, and the observed ionization bands were assigned by comparison with the results of DFT calculations. Whereas the B3LYP exchange-correlation functional provided orbital energies that permitted a preliminary assignment by application of Koopman's theorem, a more-accurate interpretation was established by calculation of the vertical ionization energies with the PW91 functional and analysis of the correlation of energy levels along the homologous series. This strategy clarified earlier disagreements in the assignment of the spectrum of benzo-2,1,3-thiadiazole.

## Introduction

There is a long-standing interest in the study of molecules that contain organic heterocycles of nitrogen and one of the chalcogens (sulfur, selenium, or tellurium) due to their many actual and proposed applications, in addition to their sometimes unusual chemistry. In the case of the 1,2,5-chalcogenadiazole ring, the sulfur derivatives can be used in antibacterial[1] and antiviral[2–7] agents, insecticides,[8] fungicides,[9] specialized polymers,[10–13] and organic LEDs;[12,14–16] the corresponding selenium compounds are also applicable as antibacterials,[13] fungicides,[9,17] and insecticides[8,17,18] in addition to dyes.[19–21] All three benzo-2,1,3-chalcogenadiazoles have been investigated as building blocks in supramolecular design because of their propensity to associate through secondary bonding interactions.[22–24]

* To whom correspondence should be addressed. vargas@chemistry.mcmaster.ca, Phone: 1-905-525-9140 ext. 23497, Fax: 1-905-522-2509.
[†] McMaster University.
[‡] The University of Arizona.

(1) Yoshida, Y.; Matsuda, K.; Sasaki, H.; Matsumoto, Y.; Matsumoto, S.; Tawara, S.; Takasugi, H. *Bioorg. Med. Chem.* **2000**, *8* (9), 2317–2335.
(2) Hanasaki, Y.; Watanabe, H.; Katsuura, K.; Takayama, H.; Shirakawa, S.; Yamaguchi, K.; Sakai, S. i.; Ijichi, K.; Fujiwara, M. *J. Med. Chem.* **1995**, *38* (12), 2038–2040.
(3) Hanasaki, Y.; Fujiwara, M.; Ide, T.; Watanabe, H.; Katsuura, K. *Toso Kenkyu Hokoku* **1996**, *40*, 3–11.
(4) Ijichi, K.; Fujiwara, M.; Hanasaki, Y.; Katsuura, K.; Shigeta, S.; Konno, K.; Yokota, T.; Baba, M. *Biochem. Mol. Biol. Int.* **1996**, *39* (1), 41–52.
(5) Ijichi, K.; Fujiwara, M.; Nagano, H.; Matsumoto, Y.; Hanasaki, Y.; Ide, T.; Katsuura, K.; Takayama, H.; Shirakawa, S., et al. *Antiviral Res.* **1996**, *31*, (1,2), 87–94.
(6) Fujiwara, M.; Ijichi, K.; Hanasaki, Y.; Ide, T.; Katsuura, K.; Takayama, H.; Aimi, N.; Shigeta, S.; Konno, K., et al. *Microbiol. Immunol.* **1997**, *41*, (4), 301–308.
(7) Fujiwara, M.; Kodama, E. N.; Okamoto, M.; Tokuhisa, K.; Ide, T.; Hanasaki, Y.; Katsuura, K.; Takayama, H.; Aimi, N.; Mitsuya, H.; Shigeta, S.; Konno, K.; Yokota, T.; Baba, M. *Antiviral Chem. Chemother.* **1999**, *10* (6), 315–320.
(8) Belen'kaya, I. A.; Prokhorchuk, E. A.; Uskova, L. A.; Shulla, T. A.; Sirik, S. A.; Goritskaya, E. F.; Grib, O. K. *Fiziologicheski Aktivnye Veshchestva* **1989**, *21*, 52–56.
(9) Belen'kaya, I. A.; Umarov, A. A.; Khamidov, M. K.; Kozyr, I. M.; Berezovskaya, E. A.; Shulla, T. A.; Sirik, S. A. *Fiziologicheski Aktivnye Veshchestva* **1990**, *22*, 47–52.
(10) Dhanabalan, A.; van Dongen, J. L. J.; van Duren, J. K. J.; Janssen, H. M.; van Hal, P. A.; Janssen, R. A. J. *Macromolecules* **2001**, *34* (8), 2495–2501.
(11) Parrini, P. *Desalination* **1983**, *48* (1), 67–78.
(12) Luo, J.; Hou, Q.; Chen, J.; Cao, Y. *Synth. Met.* **2006**, *156* (5−6), 470–475.
(13) Wang, G.; Phan, L. T.; Or, Y. S.; Qiu, Y.-L.; Niu, D.; Peng, Y.; Busuyek, M.; Wang, Y.; Nakajima, S. *Preparation of 6−11 Bridged Oxime Erythromycin Derivatives for Use as Antibacterial and Antibiotic Prodrugs*, WO/2006/119313, May 02, 2006.
(14) Tian, R.; Yang, R.; Peng, J.; Cao, Y. *Synth. Met.* **2003**, *135−136*, 177–178.
(15) Huang, J.; Niu, Y.; Xu, Y.; Hou, Q.; Yang, W.; Mo, Y.; Yuan, M.; Cao, Y. *Synth. Met.* **2003**, *135−136*, 181–182.
(16) Neto, B. A. D.; Lopes, A. S. A.; Ebeling, G.; Goncalves, R. S.; Costa, V. E. U.; Quina, F. H.; Dupont, J. *Tetrahedron* **2005**, *61* (46), 10975–10982.
(17) Belen'kaya, I. A.; Sirik, S. A.; Yasinskaya, O. G.; Ivanova, V. V.; Krokhina, G. P.; Shashenkova, D. K.; Prokhorchuk, E. A.; Uskova, L. A.; Grib, O. K. *Fiziologicheski Aktivnye Veshchestva* **1992**, *24*, 39–44.
(18) Kochansky, J. P.; Cohen, C. F.; Lusby, W. R.; Svoboda, J. A.; Feldmesser, J.; Wright, F. C. *J. Agr. Entomol.* **1988**, *5* (2), 131–137.
(19) Bazan, G. C.; Liu, B. *Methods and Compositions for Aggregant Detection*, WO/2006/083932, January 31, 2006.
(20) Pasquier, C.; Charriere, V.; Braun, H.-J. *Hair Dyes Containing Benzoxadiazole, Benzothiadiazole and Benzo-selenadiazole Derivatives*, WO/2002/022093, June 29, 2002.



10.1021/ic800055c CCC: $40.75 
Published on Web 06/21/2008

**Chart 1**

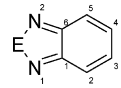

**1** E=O
**2** E=S
**3** E=Se
**4** E=Te

This has motivated multiple investigations of the electronic structures of such heterocycles, intended to better understand and improve the properties of the compounds. The accuracy of quantum mechanical calculations for these systems, especially for the derivatives of selenium and tellurium, has been limited by the size of the available basis sets, the inclusion of electron correlation (HF), the choice of exchange-correlation functional (DFT) and the inclusion of relativistic effects. Experimental verification of calculated electronic structures can in principle be obtained from the ionization potentials measured by ultraviolet photoelectron spectroscopy (UPS). Whereas the exact physical meaning of the Kohn−Sham molecular orbitals (KSMOs) is still a matter of discussion,[25,26] recent studies suggest that not only do their compositions allow for accurate bonding analyses,[27] but also their orbital energies approximate reasonably well the vertical ionization potentials (VIPs).[28]

Early UPS studies of the benzothiadiazole **2** and benzoselenadiazole **3** (Chart 1) interpreted the spectra with the assistance of semiempirical[29–32] and ab initio[33] calculations, but some assignments are ambiguous and there are disagreements in the order of the molecular orbitals. Although it can be argued that a rigorous ab initio calculation must be more accurate, unambiguous assignments can in principle be accomplished by the study of a series of at least three isoelectronic molecules. An earlier attempt[30] along these lines included the oxadiazole **1** together with **2** and **3**; however, the high electronegativity of oxygen reverses the polarity of the E−N bond changing drastically the MO structure and thus precluding definitive assignments.

Here, we present the ultraviolet photoelectron spectra of **2**, **3**, and their analogue **4** and compare them to the results of relativistic DFT calculations with different exchange-correlation functionals, in an attempt to clarify the details of their electronic structure and benchmark the computational method that has previously been employed to rationalize the solid-state structures of these systems.[24]

## Experimental Section

**Materials.** Benzo-2,1,3-thiadiazole was purchased from Aldrich, and the other heterocycles were prepared from *o*-phenylenediamine by reaction with selenium dioxide[34] or $TeCl_4$.[24] The samples were stored and handled under nitrogen; each was rigorously purified by sublimation before use.

**Instrumentation.** Photoelectron spectra were recorded with an in-house-built instrument featuring a 36 cm hemispherical analyzer (McPherson), custom-designed sample cells, and detection and control electronics. The electron detection and instrument operation are interfaced to a National Instruments PCIe-6259 multifunction data acquisition card and custom software. The samples were ionized with He I radiation (21.21 eV), the $^2E_{1/2}$ ionization of methyl iodide (9.538 eV) was used for calibration of the ionization-energy scale, and the Ar $^2P_{3/2}$ ionization (15.759 eV) was used as the internal energy scale lock during collection. The instrument resolution (measured using fwhm of the argon $^2P_{3/2}$ peak) was 0.020 eV during data collection. The sample cells were placed in the instrument and collected at the temperature (monitored with a k-type thermocouple passed through a vacuum feed-through and attached directly to the sample cell) at which the sample produced sufficient vapor pressure ($\geq 10^{-4}$ Torr) for measurements: 25 °C for both benzo-2,1,3-thiadiazole and benzo-2,1,3-selenadiazole; and 60−90 °C in 10 °C increments for benzo-2,1,3-telluradiazole.

**Data Analysis.** All data are intensity corrected with an experimentally determined instrument analyzer sensitivity function that assumes a linear dependence of analyzer transmission (intensity) to the kinetic energy of the electrons within the energy range of these experiments. The ionization bands were fitted to asymmetric Gaussian peaks over a three point baseline.[35] The bands were defined by their position, amplitude, half-width for the high binding energy side of the peak, and the half-width for the low-binding-energy side of the peak. The peak positions and half-widths were reproducible to about ±0.02 eV ($3\sigma$ level). The fitting procedures used in this work are described in more detail elsewhere.[35]

**Computational Details.** The structures considered in this study were fully optimized using the *ADF DFT* package (version 2005.01).[36–38] The adiabatic local density approximation (ALDA)


(21) Umbricht, G.; Braun, H.-J.; Oberson, S.; Mueller, C. *Two-Component Direct Hair Dyes*, DE/2001/10114426, March 24, 2002.
(22) Suzuki, T.; Fujii, H.; Yamashita, Y.; Kabuto, C.; Tanaka, S.; Harasawa, M.; Mukai, T.; Miyashi, T. *J. Am. Chem. Soc.* **1992**, *114*, 3034.
(23) Cozzolino, A. F.; Vargas-Baca, I.; Mansour, S.; Mahmoudkhani, A. H. *J. Am. Chem. Soc.* **2005**, *40* (16), 4966–4971.
(24) Cozzolino, A. F.; Britten, J. F.; Vargas-Baca, I. *Cryst. Growth Des.* **2006**, *6* (1), 181–186.
(25) Hohenberg, P.; Kohn, W. *Phys. Rev.* **1964**, *136*, B864.
(26) Kohn, W.; Sham, L. J. *Phys. Rev.* **1965**, *140*, A1133.
(27) Zhang, G.; Musgrave, C. B. *J. Phys. Chem. A* **2007**, *111* (8), 1554–1561.
(28) Chong, D. P.; Gritsenko, O. V.; Baerends, E. J. *J. Chem. Phys.* **2002**, *116* (5), 1760–1772.
(29) Johnstone, R. A. W.; Mellon, F. A. *J. Chem. Soc., Faraday Trans. 2* **1973**, *69*, 1155–1163.
(30) Clark, P. A.; Gleiter, R.; Heilbronner, E. *Tetrahedron* **1973**, *29*, 3085–3089.
(31) Petrachenko, N. E.; Vovna, V. I.; Zibarev, A. V.; Furin, G. G. *Khim. Geterotsikl. Soedin.* **1991**, (4), 563–567.
(32) Hitchcock, A. P.; Dewitte, R. S.; Vanesbroeck, J. M.; Aebi, P.; French, C. L.; Oakley, R. T.; Westwood, N. P. C. *J. Electron Spectrosc. Relat. Phenom.* **1991**, *57* (2), 165–187.
(33) Palmer, M. H.; Kennedy, S. M. F. *J. Mol. Struct.* **1978**, *43*, 33–48.
(34) Harvey, I. W.; Mcfarlane, M. D.; Moody, D. J.; Smith, D. M. *J. Chem. Soc., Perkin Trans. 1* **1988**, (7), 1939–1943.
(35) Lichtenberger, D. L.; Copenhaver, A. S. *J. Electron Spectrosc. Relat. Phenom.* **1990**, *50* (4), 335–352.
(36) Te Velde, G.; Bickelhaupt, F. M.; Baerends, E. J.; Fonseca Guerra, C.; Van Gisbergen, S. J. A.; Snijders, J. G.; Ziegler, T. *J. Comput. Chem.* **2001**, *22* (9), 931–967.
(37) Guerra, C. F.; Snijders, J. G.; Velde, G. t.; Baerends, E. J. *Theor. Chim. Acta* 1998, *99*, 391.
(38) Baerends, E. J.; Autschbach, J.; Bérces, A.; Bo, C.; Boerrigter, P. M.; Cavallo, L.; Chong, D. P.; Deng, L.; Dickson, R. M.; Ellis, D. E.; Fan, L.; Fischer, T. H.; Guerra, C. F.; Gisbergen, S. J. A. v.; Groeneveld, J. A.; Gritsenko, O. V.; Grüning, M.; Harris, F. E.; Hoek, P. v. d.; Jacobsen, H.; Kessel, G. v.; Kootstra, F.; Lenthe, E. v.; McCormack, D. A.; Osinga, V. P.; Patchkovskii, S.; Philipsen, P. H. T.; Post, D.; Pye, C. C.; Ravenek, W.; Ros, P.; Schipper, P. R. T.; Schreckenbach, H. G.; Snijders, J. G.; Sola, M.; Swart, M.; Swerhone, D.; Velde, G. t.; Vernooijs, P.; Versluis, L.; Visser, O.; Wezenbeek, E. v.; Wiesenekker, G.; Wolff, S. K.; Woo, T. K.; Ziegler, T., *ADF 2004.01; SCM, Theoretical Chemistry*; Vrije Universiteit.; Amsterdam, The Netherlands, http://www.scm.com.

was used for the exchange-correlation kernel,[39,40] and the differentiated static LDA expression was used with the Vosko−Wilk−Nusair parametrization.[41] The calculation of model geometries was gradient-corrected with the exchange and correlation functionals of the gradient correction proposed in 1991 by Perdew and Wang (PW91).[42,43] Preliminary geometry optimizations were conducted using a small double-$\zeta$ basis set with frozen cores corresponding to the configuration of the preceding noble gas and no polarization functions; the resulting structures were refined using a triple all-electron basis set with one polarization function and applying the zero-order relativistic approximation (ZORA)[44–48] formalism with the specially adapted basis sets. The $C_{2v}$ point group was used as a symmetry constraint for each molecule. Frequency calculations were performed to ensure that each geometry was at a minumum.[49,50] Single-point calculations were performed on the neutral molecule with the exchange correlation functionals proposed by Becke and Perdew (BP86),[42,51] and the statistical averaging of potentials (SAOP)[52–54] as well as B3LYP[55–57] for hybrid DFT. Single-point calculations were performed on ionized species in the neutral geometry by removing an electron from an orbital of specified symmetry using both PW91 and B3LYP.

## Results and Discussion

**Calculated Geometries.** The molecular structures were optimized using the PW91 GGA exchange-correlation functional, which is known to provide accurate results for many heavy-main-group systems. These models correspond to the structures of individual molecules in the gas phase and are appropriate for the interpretation of the photoelectron spectra. However, the experimental data available for comparison of geometries proceed only from crystallographic determinations of single crystals,[24,58,59] in which intermolecular association can induce significant structural changes.[23,24] The optimized molecular dimensions were comparable to the crystallographic measurements (within less than three times the standard deviation) for the benzene rings. The five-membered rings of **2** and **3** showed somewhat larger deviations; the tellurium heterocycle had good agreement in bond lengths but large deviations in bond angles. It is precisely in the last case that the strong secondary bonding interactions alter the free-molecule geometry; better molecular dimensions are obtained with models of associated molecules.[24]

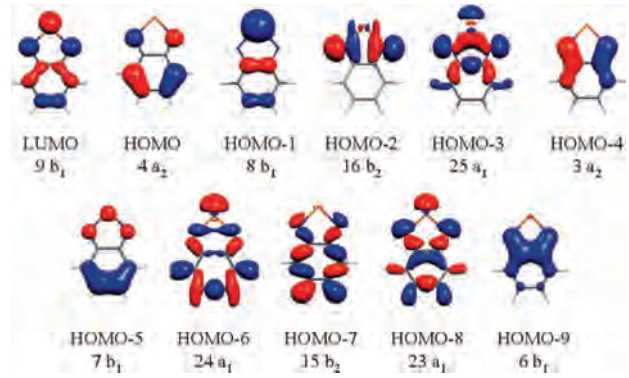


**Figure 1.** LUMO and the 10 highest-occupied molecular orbitals of benzo-2,1,3-telluradiazole, **4**. Isosurfaces plotted at 0.05.

**MO Compositions.** The electronic structure of the benzochalcogenadiazoles was calculated using three GGA and one hybrid exchange-correlation potentials: BP86 which has been commonly used with ADF, PW91 which usually provides better structural parameters for heavy main-group systems; SAOP which is usually recommended for TD-DFT calculations and has been recently proposed for the assignment of photoelectron spectra;[28] and the popular B3LYP. Atomic contributions to the molecular orbitals are dependent on the nature of the chalcogen but, for each molecule, the composition of the KSMOs determined with all four methods is essentially identical. The energies and the order of the inner orbitals show small variations between functionals. Figure 1 displays the calculated composition of the LUMO and the 10 most-external orbitals of **4**, which correspond to the electrons that are most easily removed: those in the $\pi$ manifold and the lone-pairs. The $C_{2v}$ symmetry allows the distinction of $\pi$ ($a_2$, $b_1$) and $\sigma$ ($a_1$, $b_2$) orbitals. The calculated LUMO ($b_1$) is a $\pi$ orbital with 4 nodal planes and predominantly chalcogen-nitrogen antibonding character. The composition of the HOMO ($a_2$ symmetry) corresponds to electron density on the C═C bonds in the Lewis structure and has less than 2% chalcogen character in all three cases. The HOMO-1 ($b_1$) is primarily the chalcogen $\pi$ lone pair (sulfur: 33%, selenium: 48%, tellurium: 62%). The HOMO-2 ($b_2$) and HOMO-3 ($a_1$) are both $\sigma$ orbitals that represent the in-phase and out-of-phase combinations of the nitrogen lone pairs; the HOMO-3 also contains a significant contribution from the chalcogen $\sigma$ lone pair (sulfur: 8%, selenium: 16%, tellurium: 23%). The HOMO-4 ($a_2$) and HOMO-5 ($b_1$) are $\pi$-orbitals with 2 nodal planes each. The small overlap in

(39) van Gisbergen, S. J. A.; Snijders, J. G.; Baerends, E. J. *Phys. Rev. Lett.* **1997**, *78* (16), 3097–3100.
(40) van Gisbergen, S. J. A.; Snijders, J. G.; Baerends, E. J. *J. Chem. Phys.* **1998**, *109* (24), 10644–10656.
(41) Vosko, S. H.; Wilk, L.; Nusair, M. *Can. J. Phys.* **1980**, *58* (8), 1200–1211.
(42) Perdew, J. P. *Phys. Rev. B: Condens. Matter* **1986**, *33*, 8822.
(43) Perdew, J. P.; Wang, Y. *Phys. Rev. B: Condens. Matter Mater. Phys.* **1992**, *45*, 13244.
(44) van Lenthe, E.; Ehlers, A.; Baerends, E.-J. *J. Chem. Phys.* **1999**, *110* (18), 8943–8953.
(45) van Lenthe, E.; Baerends, E. J.; Snijders, J. G. *J. Chem. Phys.* **1993**, *99* (6), 4597–4610.
(46) van Lenthe, E.; Baerends, E. J.; Snijders, J. G. *J. Chem. Phys.* **1994**, *101* (11), 9783–9792.
(47) van Lenthe, E.; Snijders, J. G.; Baerends, E. J. *J. Chem. Phys.* **1996**, *105* (15), 6505–6516.
(48) van Lenthe, E.; van Leeuwen, R.; Baerends, E. J.; Snijders, J. G. *Int. J. Quantum Chem.* **1996**, *57* (3), 281–293.
(49) Fan, L. Y.; Ziegler, T. *J. Phys. Chem.* **1992**, *96* (17), 6937–6941.
(50) Fan, L. Y.; Ziegler, T. *J. Chem. Phys.* **1992**, *96* (12), 9005–9012.
(51) Becke, A. D. *Phys. Rev. A* **1988**, *38* (6), 3098–3100.
(52) Gritsenko, O. V.; Schipper, P. R. T.; Baerends, E. J. *Chem. Phys. Lett.* **1999**, *302* (3−4), 199–207.
(53) Gritsenko, O. V.; Schipper, P. R. T.; Baerends, E. J. *Int. J. Quantum Chem.* **2000**, *76* (3), 407–419.
(54) Schipper, P. R. T.; Gritsenko, O. V.; van Gisbergen, S. J. A.; Baerends, E. J. *J. Chem. Phys.* **2000**, *112* (3), 1344–1352.
(55) Lee, C. T.; Yang, W. T.; Parr, R. G. *Phys. Rev. B: Condens. Matter Mater. Phys.* **1988**, *37* (2), 785–789.
(56) Becke, A. D. *J. Chem. Phys.* **1993**, *98* (7), 5648–5652.
(57) Stephens, P. J.; Devlin, F. J.; Chabalowski, C. F.; Frisch, M. J. *J. Phys. Chem.* **1994**, *98* (45), 11623–11627.
(58) Suzuki, T.; Tsuji, T.; Okubo, T.; Okada, A.; Obana, Y.; Fukushima, T.; Miyashi, T.; Yamashita, Y. *J. Org. Chem.* **2001**, *66* (26), 8954–8960.
(59) Gomes, A. C.; Biswas, G.; Banerjee, A.; Duax, W. L. *Acta Crystallogr., Sect. C* **1989**, *45*, 73–75.

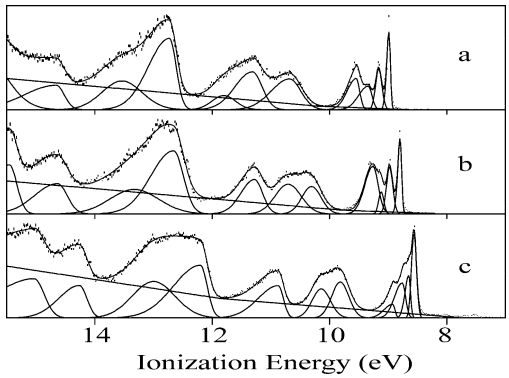


**Figure 2.** Photoelectron spectra of (a) **2**, (b) **3**, and (c) **4**.

the HOMO-5 between the chalcogen and nitrogen, the chalcogen contribution to this orbitals decreases down the group (sulfur: 18%, selenium: 17%, tellurium: 12%). The HOMO-6 and HOMO-7 are $\sigma$ orbitals with symmetries $a_1$ and $b_2$ respectively, which swap order in the case of **3**. The $a_1$ orbital contains chalcogen $\sigma$ lone pair character (S: 46%, Se: 21%, Te: 19%). The HOMO-8 ($a_1$) is also part of the sigma framework with chalcogen $\sigma$ lone pair character (sulfur: 6%, selenium: 16%, tellurium: 13%). The HOMO-9 (HOMO-10 for **2**) is the lowest-energy $\sigma$ orbital, it has a $b_1$ symmetry with one node, and its chalcogen contribution decreases for the heavier molecules (sulfur: 27%, selenium: 13%, tellurium: 6%). Overall, the electronic structures display increasing localization of electron density as the $\sigma$ overlap between nitrogen and the chalcogen becomes less efficient; indeed the crystal structures of these compounds do show a high degree of bond alternation.[24,60]

**He I Photoelectron Spectra.** The acquired photoelectron spectra of the benzo-2,1,3-chalcogenadiazoles **2**−**4** are displayed in Figure 2, and the vertical length of each data point corresponds to the experimental variance.[35] The spectrum of **2** is consistent with those recorded previously,[30–33] consisting of three groups of overlapping bands between 8 and 10 eV, 10 and 12 eV, as well as between 12 and 14 eV. The spectra of the heavier **3** and **4** display similar patterns, shifted to lower energies. There are two previous reports of the spectrum of **3**[31,33] but none of the photoelectron spectrum of **4**; in the latter the second set of bands is split in two.

For the spectrum of **2**, the bands between 10 and 12 eV were modeled with three asymmetric Gaussian envelopes while the bands between 12 and 14 eV required two asymmetric Gaussian envelopes. The measured vertical ionization energies for each model band are given in Table 1 and are compared with those determined in previous studies; most values agree within 0.04 eV but there are a few exceptions. The first group of bands corresponds to ionization from the two most-external orbitals only, the first of which displays vibrational structure that is fit with a progression of three Gaussians in each spectrum. An earlier report[29] lists the second ionization energy as 9.65 eV, 0.11 eV above the value observed in this work, another peak was reported at 12.38 eV but this corresponds to the bottom of a valley between two bands in the present study; the disagreement is possibly the result of a typographical error. Three reports list an ionization shoulder at 11.6 eV[30] or 11.7 eV,[31,32] which must correspond to the band fitted at 11.84 eV.

**Table 1.** Experimental VIPs and Assignments for **2**, **3**, and **4** in eV

| **2** | | | | | | Assignment | | | |
|---|---|---|---|---|---|---|---|---|---|
| IE[a] | IE[b] | IE[c] | IE[d] | IE[e] | IE[f] | *a* | *b* | *c* | *f* |
| 8.98 | 9.00 | 8.98 | 9.00 | 8.95 | 9.00 | $a_2$ ($\pi$) | $a_2$ ($\pi$) | $a_2$ ($\pi$) | $a_2$ ($\pi$) |
| 9.54 | 9.55 | 8.95 | 9.65 | 9.50 | 9.56 | $b_1$ ($\pi$) | $b_1$ ($\pi$) | $b_1$ ($\pi$) | $b_1$ ($\pi$) |
| 10.68 | 10.71 | 9.52 | 10.71 | 10.66 | 10.69 | $b_2$ ($\sigma$) | $b_2$ ($\sigma$) | $a_1$ ($\sigma$) | $b_2$ ($\sigma$) |
| 11.31 | 11.32 | 10.64 | 11.27 | 11.32 | 11.28 | $a_1$ ($\sigma$) | $a_2$ ($\pi$) | $a_2$ ($\pi$) | $a_2$ ($\pi$) |
| | | 11.31 | | | | $a_2$ ($\pi$) | $a_1$ ($\sigma$) | | |
| 11.80 | | | | 11.7[g] | 11.70 | $b_1$ ($\pi$) | $b_1$ ($\pi$) | $b_2$ ($\sigma$) | $a_1$ ($\sigma$) |
| 12.73 | 12.83 | 11.6[g] | 12.38 | 12.74 | 12.78 | $a_1$ ($\sigma$) | $a_1$ ($\sigma$) | | $b_1$ ($\pi$) |
| | | | | | | $b_2$ ($\sigma$) | $b_2$ ($\sigma$) | | |
| | | | | | | $a_1$ ($\sigma$) | $a_1$ ($\sigma$) | | |
| **3** | | | | | | Assignment | | | |
| IE[a] | IE[b] | | | | IE[f] | *a* | b | | *f* |
| 8.80 | 8.81 | | | | 8.76 | $a_2$ ($\pi$) | $a_2$ ($\pi$) | | $a_2$ ($\pi$) |
| 9.26 | 9.30 | | | | 9.24 | $b_1$ ($\pi$) | $b_1$ ($\pi$) | | $b_1$ ($\pi$) |
| 10.30 | 10.55 | | | | 10.36 | $b_2$ ($\sigma$) | $b_2$ ($\sigma$) | | $b_2$ ($\sigma$) |
| 10.70 | | | | | 10.62 | $a_1$ ($\sigma$) | $a_2$ ($\pi$) | | $a_2$ ($\pi$) |
| | | | | | | $a_2$ ($\pi$) | $a_1$ ($\sigma$) | | |
| 11.27 | 11.30 | | | | 11.25 | $b_1$ ($\pi$) | $b_1$ ($\pi$) | | $a_1$ ($\sigma$) |
| 12.66 | 12.85 | | | | 12.41 | $b_2$ ($\sigma$) | $a_1$ ($\sigma$) | | $b_1$ ($\pi$) |
| | | | | | 12.76 | $a_1$ ($\sigma$) | $b_2$ ($\sigma$) | | $a_1$ ($\sigma$) |
| | | | | | | $a_1$ ($\sigma$) | $a_1$ ($\sigma$) | | |
| **4** | | | | | | Assignment | | | |
| IE[a] | | | | | | *a* | | | |
| 8.57 | | | | | | $a_2$ ($\pi$) | | | |
| 8.92 | | | | | | $b_1$ ($\pi$) | | | |
| 9.82 | | | | | | $b_2$ ($\sigma$) | | | |
| 10.14 | | | | | | $a_1$ ($\sigma$) | | | |
| | | | | | | $a_2$ ($\pi$) | | | |
| 10.87 | | | | | | $b_1$ ($\pi$) | | | |
| 12.20 | | | | | | $a_1$ ($\sigma$) | | | |
| | | | | | | $b_2$ ($\sigma$) | | | |
| | | | | | | $a_1$ ($\sigma$) | | | |

[a] This work, see the end of discussion for justification. [b] Ref 33. [c] Ref 30. [d] Ref 29. [e] Ref 32. [f] Ref 31. [g] Shoulder.

Compared to the spectrum of **2**, the photoelectron spectrum of **3** displays the most conspicuous differences in the second set of peaks. The sharp features of this spectrum correspond within 0.08 eV to the previously reported values (Table 1).[31,33] In the first study, the feature between 9.8 and 11 eV was attributed to a single ionization, the new determination resolves clearly two bands and corresponds well with the second study. There is also disagreement in the position of the ionization at 12.66 eV, but the peak fitting method employed in the present study is more accurate in the characterization of peaks with poorly defined maxima.

**Spectral Assignments.** Successful matching of electronic structure calculations with the photoelectron spectrum of a molecule requires agreement in both the values of the ionization energies and the nature of the corresponding molecular orbitals. As a first approximation, assignments of the experimental spectra from the calculated electronic structures can be attempted by application of Koopman's theorem, bearing in mind that such an approach does not account for correlation or relaxation upon electron removal. One more fundamental issue is that KSMOs are inherently different from those obtained by HF methods. Fortunately, recent investigations have shown that it is possible to correlate the DFT orbital energies with the vertical ionization potentials[28] as long as a correction is introduced to account

(60) Chivers, T.; Gao, X. L.; Parvez, M. *Inorg. Chem.* **1996**, *35* (1), 9–15.

**Table 2.** Koopman's Theorem Ionization Energies in eV, Calculated Vertical Ionization Potentials in eV and Corresponding Orbital Symmetries for **2**, **3**, and **4**

| | Benzo-2,1,3-thiadiazole (**2**) | | | | | |
|---|---|---|---|---|---|---|
| | Koopman's Theorem Energies | | | | VIPs | |
| | PW91 | SAOP | BP86 | B3LYP | PW91 | B3LYP |
| $a_2$ ($\pi$) | 8.97 | 9.02 | 8.96 | 8.96 | 9.08 | 9.32 |
| $b_1$ ($\pi$) | 9.49 | 9.45 | 9.48 | 9.49 | 9.53 | 9.87 |
| $b_2$ ($\sigma$) | 10.09 | 10.27 | 10.09 | 10.63 | 10.80 | 11.55 |
| $a_1$ ($\sigma$) | 10.64 | 10.65 | 10.64 | 11.17 | 10.84 | 11.56 |
| $a_2$ ($\pi$) | 11.09 | 11.16 | 11.08 | 11.35 | 11.47 | 11.92 |
| $b_1$ ($\pi$) | 11.73 | 11.73 | 11.73 | 12.05 | 11.84 | 12.42 |
| $a_1$ ($\sigma$) | 12.18 | 12.10 | 12.09 | 12.64 | | 13.22 |
| $b_2$ ($\sigma$) | 12.26 | 12.18 | 12.18 | 12.85 | | |
| $a_1$ ($\sigma$) | 12.44 | 12.40 | 12.26 | 13.05 | | |
| | Benzo-2,1,3-selenadiazole (**3**) | | | | | |
| | Koopman's Theorem Energies | | | | VIPs | |
| | PW91 | SAOP | BP86 | B3LYP | PW91 | B3LYP |
| $a_2$ ($\pi$) | 8.79 | 8.82 | 8.79 | 8.79 | 8.85 | 9.10 |
| $b_1$ ($\pi$) | 9.23 | 9.15 | 9.23 | 9.22 | 9.32 | 9.58 |
| $b_2$ ($\sigma$) | 9.90 | 10.02 | 9.90 | 10.38 | 10.34 | 11.04 |
| $a_1$ ($\sigma$) | 10.23 | 10.17 | 10.23 | 10.69 | 10.51 | 11.15 |
| $a_2$ ($\pi$) | 10.96 | 10.99 | 10.96 | 11.23 | 11.24 | 11.70 |
| $b_1$ ($\pi$) | 11.37 | 11.33 | 11.37 | 11.66 | 11.43 | 11.98 |
| $a_1$ ($\sigma$) | 12.18 | 12.05 | 12.18 | 12.62 | | 12.93 |
| $b_2$ ($\sigma$) | 12.15 | 12.04 | 12.15 | 12.74 | | |
| $a_1$ ($\sigma$) | 12.30 | 12.26 | 12.31 | 12.90 | | |
| | Benzo-2,1,3-telluradiazole (**4**) | | | | | |
| | Koopman's Theorem Energies | | | | VIPs | |
| | PW91 | SAOP | BP86 | B3LYP | PW91 | B3LYP |
| $a_2$ ($\pi$) | 8.59 | 8.51 | 8.59 | 8.59 | 8.59 | 8.84 |
| $b_1$ ($\pi$) | 8.83 | 8.61 | 8.84 | 8.77 | 8.86 | 9.11 |
| $b_2$ ($\sigma$) | 9.55 | 9.53 | 9.56 | 9.96 | 9.74 | 10.36 |
| $a_1$ ($\sigma$) | 9.66 | 9.50 | 9.68 | 10.05 | 10.02 | 10.61 |
| $a_2$ ($\pi$) | 10.80 | 10.71 | 10.80 | 11.07 | 10.99 | 11.45 |
| $b_1$ ($\pi$) | 11.00 | 10.88 | 11.01 | 11.27 | 11.01 | 11.54 |
| $a_1$ ($\sigma$) | 11.89 | 11.64 | 11.89 | 12.33 | | 12.54 |
| $b_2$ ($\sigma$) | 11.93 | 11.71 | 11.94 | 12.52 | | |
| $a_1$ ($\sigma$) | 12.14 | 11.99 | 12.15 | 12.73 | | |

for a systematic error that is unique to each exchange-correlation functional.[61] Empirical correction factors were obtained by averaging the difference between the energy of the HOMO and the first measured ionization band for all three compounds; these correction factors are −2.77 eV for PW91, 1.29 eV for SAOP, −2.72 for BP86, and −2.14 for B3LYP and were used to offset the orbital energies calculated with each functional. The DFT orbital energies corrected in this way are given in Table 2. The values obtained from calculations with the gradient-corrected functionals BP86, PW91 and SAOP are close to each other. The maximum differences of BP86 from PW91 are 0.18, 0.01, and 0.02 eV for **2**, **3**, and **4** respectively. The corresponding SAOP differences are 0.18, 0.13, and 0.25 eV; and 0.61, 0.60, and 0.59 eV for B3LYP. The first two ionizations match well the corrected energies of the HOMO and the HOMO-1, within 0.1 eV for all functionals, with exception of the SAOP HOMO-2 of **4**. Subsequent bands cannot be assigned because individual ionization processes are not resolved.

To obtain more reliable assignments than those based on Koopman's theorem alone, relaxation can be accounted for

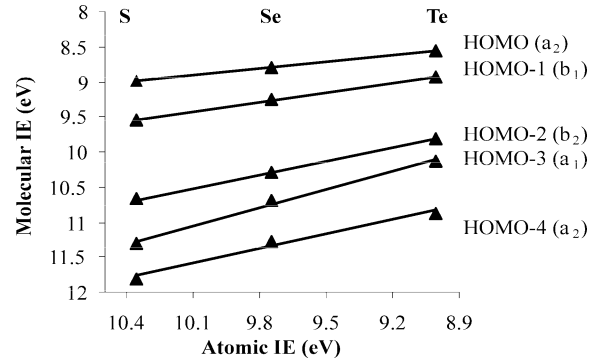


**Figure 3.** Experimental ionization energies of the benzo-2,1,3-chalcogenadiazoles, **2**−**4,** correlated to the first ionization potential of the respective chalcogen.

by calculating the vertical ionization potentials as the energy difference between ground and the ionized states evaluated by removal of one electron from a particular orbital from the molecule in the ground-state geometry (eq 1). The vertical ionization potentials calculated with PW91 and B3LYP are reported with no further correction in Table 2. There are significant differences between the VIPs calculated by these functionals. B3LYP overestimates the ionization energies by between 0.24 and 0.75 eV as compared to PW91. The VIPs calculated with PW91 agree with the experimental VIPs within 0.10, 0.06, and 0.06 eV for the first two orbitals of **2**, **3**, and **4**, respectively. However, this approach alone cannot conclusively assign the next bands.

$$\mathrm{VIP} = \mathrm{E(h)} - \mathrm{E(e^-)} = \mathrm{E(M^+)} - \mathrm{E(M)} \qquad (1)$$

Further insight into the identity of the inner orbitals, from which each of the next ionization bands originate, can be obtained by comparison of the spectra of the three benzo-2,1,3-chalcogenadiazoles. Because all of the members of this family should have valence orbitals of similar composition and energy order, the ionization energies should decrease as the atomic number of the chalcogen increases and the trend should be almost linear, as in the cases of the dimethyl chalcogenides ($(CH_3)_2E$, E = S, Se, Te),[62] the pnictabenzenes (P, As, Sb),[63] and the triphenyl derivatives of groups 14[64] and 15[65] elements. Figure 3 presents the experimentally determined and calculated ionization potentials as a function of the first ionization potential of the chalcogen atoms.[66] Approximately linear trends are observed for several orbital/ionization energies and can be quantitatively characterized by the slope and the correlation coefficient (Table 3). The linear character of the trends is stronger when the relevant molecular orbital has a greater contribution from the chalcogen and is weaker when the orbital is mostly localized in

(61) Stowasser, R.; Hoffmann, R. *J. Am. Chem. Soc.* **1999**, *121* (14), 3414–3420.
(62) Chang, F. C.; Young, V. Y.; Prather, J. W.; Cheng, K. L. *J. Electron Spectrosc. Relat. Phenom.* **1986**, *40* (4), 363–383.
(63) Batich, C.; Heilbronner, E.; Hormung, V.; Ashe III, A. J.; Clark, D. T.; Cobley, U. T.; Kilcast, D.; Scanlan, I. *J. Am. Chem. Soc.* **1973**, *95*, 928–930.
(64) Distefano, G.; Pignataro, S.; Szepes, L.; Borossay, J. *J. Organomet. Chem.* **1976**, *104* (2), 173–178.
(65) Distefano, G.; Pignataro, S.; Szepes, L.; Borossay, J. *J. Organomet. Chem.* **1975**, *102*, 313–316.
(66) Lide, D. R., *CRC Handbook of Chemistry and Physics, Internet Version 87 ed.*; Taylor and Francis: Boca Raton, FL, 2007.

**Table 3.** Slopes ($m$) and Correlation Coefficients ($R^2$) for Ionization Energies of **2**, **3**, and **4** with Atomic First Ionization Energies of Sulfur, Selenium, and Tellurium

| PES | Ionization Band | 1 | 2 | 3 | 4 | | 5 | 6 |
|---|---|---|---|---|---|---|---|---|
| | $m$ | 0.30 | 0.46 | 0.64 | 0.86 | | 0.68 | 0.40 |
| | $R^2$ | 1.00 | 1.00 | 1.00 | 1.00 | | 0.98 | 0.88 |
| Koopmans Theorem | Orbital | HOMO | HOMO-1 | HOMO-2 | HOMO-3 | HOMO-4 | HOMO-5 | HOMO-6 |
| PW91 | $m$ | 0.29 | 0.50 | 0.41 | 0.75 | 0.22 | 0.56 | 0.22 |
| | $R^2$ | 1.00 | 0.99 | 0.98 | 1.00 | 1.00 | 1.00 | 0.85 |
| BP86 | $m$ | 0.28 | 0.49 | 0.41 | 0.74 | 0.21 | 0.55 | 0.16 |
| | $R^2$ | 1.00 | 0.99 | 0.98 | 1.00 | 1.00 | 1.00 | 0.57 |
| SAOP | $m$ | 0.39 | 0.65 | 0.59 | 0.85 | 0.34 | 0.65 | 0.36 |
| | $R^2$ | 0.99 | 0.99 | 0.98 | 1.00 | 0.99 | 1.00 | 0.88 |
| B3LYP | m | 0.28 | 0.55 | 0.51 | 0.86 | 0.22 | 0.60 | 0.24 |
| | $R^2$ | 1.00 | 0.99 | 0.99 | 1.00 | 1.00 | 1.00 | 0.81 |
| VIP | Ionization | 1 | 2 | 3 | 4 | 5 | 6 | |
| PW91 | $m$ | 0.37 | 0.51 | 0.81 | 0.62 | 0.36 | 0.64 | |
| | $R^2$ | 1.00 | 0.97 | 1.00 | 1.00 | 1.00 | 1.00 | |
| B3LYP | $m$ | 0.37 | 0.59 | 0.90 | 0.72 | 0.35 | 0.67 | |
| | $R^2$ | 1.00 | 0.99 | 1.00 | 1.00 | 1.00 | 1.00 | |

the benzene rings. This analysis is limited to the first six ionizations, for which correlations are clearly defined. The slopes are also useful to confirm the assignments and, in some instances, they can clarify ambiguous assignments. For example, on the basis of only the orbital energies calculated by BP86, PW91, and SAOP, assignment of the third and fourth ionizations is ambiguous because one of the ionizations from either the HOMO-2 or the HOMO-4 is not visible. The slope magnitudes indicate that it is the HOMO-4 that does not have a distinguishable ionization band in the He I spectrum. Assignment of the third and fourth ionization to the HOMO-2 and HOMO-3 agrees with B3LYP orbital energies within 0.14, 0.08, and 0.14 eV for for **2**, **3**, and **4**, respectively. The slope magnitude, however, cannot be used as an absolute criterion to determine the nature of each molecular orbital. In the present case, the HOMO is nodal at the chalcogen and the HOMO-1 is essentially a chalcogen lone-pair, yet the slopes of their corresponding ionizations are different by 0.2 at most. On the other hand, the slope of the second ionization is comparable to that of the first electron removal from pnictabenzenes, a much steeper slope[63] is suggested by the first ionizations of the 1,2,3,5-dithia- and 1,2,3,5-diselenadiazolyl radicals.[67]

The shape of the bands, including the vibrational structure is also indicative of orbital character. The narrow first two bands are consistent with ionization from $\pi$ orbitals, for which the corresponding ionized states undergo very small geometric changes. The vibrational structure of the first ionization band (8−10 eV in the case of **2**) contains some information on the nature of the HOMO. The vibrational wavenumber measured as the distance between maxima in the vibrational progression is 1350 ± 160 cm$^{-1}$ (0.02 eV) for all three compounds **2**, **3**, and **4**. This value must correspond to an $A_1$ normal mode in a region characteristic of $\upsilon_{CC}$ and $\upsilon_{CN}$ stretching vibrations within the carbocycle and are consistent with removal of an electron from a wave function that has electron density located over the C═C and *C*═N bonds. The calculated normal mode that best fits these requirements has 1342, 1321, and 1318 cm$^{-1}$ in **2**, **3**, and **4**, respectively; experimentally, the Raman spectra displays the closest bands at 1359 for **2**,[68] 1349 for **3**,[68] and 1343 cm$^{-1}$ for **4**.[24] This interpretation of the vibrational structure is consistent with the composition of the HOMO and agrees with the previous report for **2** and **3**.[31]

The combination of VIP energies and slopes within the homologous series leads to the final assignment for ionizations observed below 13 eV that is presented in Table 1. Agreement for PW91 results is within 0.16 eV for all the ionizations in each of the molecules except for the fourth ionization of the sulfur and selenium analogues, which differs by 0.47 and 0.19 eV, respectively. Interestingly, B3LYP gave larger errors (0.19−0.87 eV). Above 13 eV for each spectrum, close spacing of orbitals precludes assignments with this approach.

**Reorganization Energy.** The solvent-independent changes of energy associated to the structural relaxation upon ionization of each molecule were determined in two steps. The first consisted in fitting the intensities of the vibrational progression to a Poisson distribution (eq 2). Here, $I$ is the intensity of the $n$th vibrational band, and $S$ is a distortion parameter. The latter parameter was then applied to eq 3, where $h$ is Planck's constant and $\lambda$ the reorganization energy.

$$I_n = \frac{S^n}{n!}e^{-s} \tag{2}$$

$$\lambda_v = \sum_k S_k h\upsilon_k \tag{3}$$

Overlap of the first and second ionizations was taken in account when modeling the vibrational progression in each spectrum. From the progression frequencies given above, the fitted distortion parameters and the corresponding reorganization energies were: 0.65, 0.11 ± 0.02 eV; 0.80, 0.13 ± 0.02 eV; and 0.60, 0.10 ± 0.02 eV for **2**, **3**, and **4**, respectively. These energy values are comparable to those calculated using PW91: 0.08, 0.09, and 0.07 eV for **2**, **3**, and **4**.

The small magnitudes of reorganization energy (c.f. 0.180 ± 0.005 eV for 1,10-phenanthroline[69] and 0.059 ± 0.004

(67) Cordes, A. W.; Bryan, C. D.; Davis, W. M.; de Laat, R. H.; Glarum, S. H.; Goddard, J. D.; Haddon, R. C.; Hicks, R. G.; Kennepohl, D. K.; Oakley, R. T.; Scott, S. R.; Westwood, N. P. C. *J. Am. Chem. Soc.* **1993**, *115*, 7232–7239.

(68) Korobkov, V. S.; Sechkarev, A. V.; Zubanova, L. P.; Dvorovenko, N. I. *Izvestiya Vuz. Fizika* **1968**, *11* (4), 158–160.

eV for pentacene[70]) together with the tendency of these molecules to form extended supramolecular structures[23,24] invite further investigations of the charge-transport properties of materials based on chalcogenadiazole heterocycles.

## Conclusions

The investigation of the photoelectron spectra of the benzo-2,1,3-chalcogenadiazole homologous series − including the sulfur, selenium, and tellurium derivatives − showed that both GGA and hybrid DFT calculations can successfully be applied in their interpretation. Although preliminary assignments can be conducted using a single point B3LYP calculation, a more-reliable identification of orbitals requires actual calculation of vertical ionization potentials and a study of the correlations of orbital energies with the first ionization potential of the chalcogen atoms.

(69) Amashukeli, X.; Winkler, J. R.; Gray, H. B.; Gruhn, N. E.; Lichtenberger, D. L. *J. Phys. Chem. A* **2002**, *106* (33), 7593–7598.
(70) Gruhn, N. E.; da Silva, D. A.; Bill, T. G.; Malagoli, M.; Coropceanu, V.; Kahn, A.; Bredas, J. L. *J. Am. Chem. Soc.* **2002**, *124* (27), 7918–7919.

**Acknowledgements.** This project has been supported by grants from the Natural Sciences and Engineering Research Council of Canada (NSERC), the Canada Foundation for Innovation (CFI), the Ontario Innovation Trust (OIT) and computational time on the Shared Hierarchical Academic Research Computing Network (SHARCNET: www.sharcnet.ca). Photoelectron spectra were collected during the ACS-PRF Summer School on Molecular Photoelectron Spectroscopy for Chemical Research and Education, June 12-15, 2005 (ACS-PRF Award 42603-H).

**Supporting Information Available:** Bond distances and angles for experimental and calculated geometries for **2**, **3**, and **4**. Molecular orbital compositions for **2**, **3**, and **4** with PW91, BP86, SAOP, and B3LYP functionals. Correlation of atomic ionization energy with calculated vertical ionization potentials (PW91 and B3LYP) for **2**, **3**, and **4**. This material is available free of charge via the Internet at http://pubs.acs.org.

IC800055C